



Technical Note

The effect of concave surface curvature on heat transfer from a fully developed round impinging jet

D.H. Lee*, Y.S. Chung, S.Y. Won

School of Mechanical and Automotive Engineering, Inje University, 607 Obang-Dong, Kimhae, Kyungnam 612-749, Korea

Received 6 February 1998; in final form 28 August 1998

Nomenclature

A surface area of the gold film Intrex
 C_p wall pressure coefficient ($= (P_w - P_\infty) / (0.5 \rho U_{ce}^2)$)
 d pipe nozzle diameter
 D inner diameter of the concave hemisphere
 d/D concave surface curvature
 h local heat transfer coefficient
 I current across the gold film Intrex
 $I.D.$ inner diameter of upstream pipe
 k thermal conductivity of air
 L nozzle-to-surface distance
 Nu local Nusselt number ($= h d/k$)
 Nu_{st} stagnation point Nusselt number
 P_w wall pressure on the concave hemisphere
 P_∞ atmospheric pressure
 q_c conduction heat loss
 q_v net heat flux
 r streamwise distance from the stagnation point
 Re Reynolds number based on mean velocity and nozzle diameter ($= Ud/v$)
 T_a ambient temperature
 T_j jet temperature
 T_w concave surface temperature measured by liquid crystal
 U_{ce} jet centerline mean velocity at the nozzle exit
 V voltage across the gold film Intrex.

Greek symbols

ε emissivity of the liquid crystal and black paint coated surface
 ν kinematic viscosity of air

ρ density of air
 σ Stefan–Boltzmann constant.

1. Introduction

Due to a high heat and mass transfer enhancement, impinging jets have been widely used in a variety of engineering applications such as cooling of hot steel plates, tempering of glass, drying of papers and films, and cooling of turbine blades and electronic components. Heat transfer studies have dealt with the effects of Reynolds number, nozzle-to-plate distance, nozzle geometry, jet temperature, target surface orientation, multiple jets, cross flow, and surface shape on the flow and heat transfer characteristics.

Several review and summary papers on the impinging jet heat transfer have been published by Martin [1], Jambunathan et al. [2] and Viskanta [3]. A great majority of impinging jet studies in the past were on a flat surface. However, many industrial applications of jet impingement cooling on a curved surface may be encountered.

A few papers have studied the impinging heat transfer from a curved surface. Chupp et al. [4] studied the heat transfer characteristics with an array of round jets impinging on a concave surface. Thomann [5] found that the heat transfer on a concave surface is around 20% higher than that on a flat surface because the concave surface curvature destabilizes the boundary layer flow and increases the intensity of the turbulent mixing, which in turn produces large scale vortices (called Taylor–Görtler vortices) with axes in the flow direction. Hrycak [6] also reported that the total heat transfer on a concave surface is higher than that on a flat plate geometry due to larger surface area, especially for small nozzle-to-surface distances. Gau and Chung [7] studied the effects of sur-

* Corresponding author.

face curvature on the two-dimensional slot jet impinging heat transfer along semi-cylindrical concave and convex surfaces. They reported that at the stagnation point region on a convex surface, the momentum transport in the flow is increased due to a series of three-dimensional counterrotating vortices initiated near the wall, and subsequently the heat transfer rate is augmented. They also found that on a concave surface, the heat transfer rate on and around the stagnation point increases with increasing surface curvature.

Yang et al. [8] investigated jet impingement cooling on a semi-circular concave surface with two different nozzles (round edged and rectangular edged nozzles). They also studied characteristics of free jets issuing from two nozzles. Most recently, Lee et al. [9] studied the effects of a hemispherically convex surface curvature on the local heat transfer by a round impinging jet issuing from a long straight pipe nozzle. They found that the stagnation point Nusselt number increases with increasing surface curvature due to an increased acceleration from the stagnation point for a higher convex surface curvature.

In the present study, the local heat transfer coefficients and the wall pressure coefficient profiles are measured for a round turbulent jet impinging on a concave hemispherical surface. This is an extension of the previous study by Lee et al. [9] on a convex hemispherical surface. The experiments are made for the jet Reynolds number (based on the pipe diameter) of $Re = 11\,000\text{--}50\,000$, nozzle-to-plate distance of $L/d = 2\text{--}10$, and surface curvature of $d/D = 0.034\text{--}0.089$. An electrically heated gold film Intrex (a thin gold-coated polyester sheet) is used to create a uniform heat flux on the surface. The surface temperature is determined using thermochromic liquid crystal and a color image processing system as a means of the quantitative color determination of the liquid crystal.

2. Test apparatus and analysis

Figure 1 shows a schematic diagram of the test apparatus, which is nearly identical to the impinging jet study by Lee et al. [9] except for the impinging surface geometry. The apparatus consists of a blower, a heat exchanger, an orifice flow meter, a cast acrylic pipe with three inner diameters of $d = 1.3, 2.15$ and 3.4 cm and three lengths of $L = 76, 125$ and 197 cm. Therefore, a fully developed round jet resulting from the development length-to-pipe diameter ratio of 58 impinges perpendicularly upon a concave hemispherical surface. A heat exchanger is used to maintain the jet temperature at the nozzle exit within $\pm 0.2^\circ\text{C}$ of the ambient temperature.

The test model consists of a 3.5 mm thick and 38.1 cm diameter Plexiglas concave hemisphere to which three 60 cm long strips (one 2.5 cm wide strip in the middle as a main heater and two 1.5 cm wide strips on both sides as

guard heaters) of the gold film Intrex are glued. An air brush is used to apply first the micro-encapsulated thermochromic liquid crystal and then black backing paint on the Intrex surface. A digital color image processing system is used to quantitatively determine the temperature corresponding to a particular color of liquid crystal. To measure the wall pressure, 25 stainless steel tubes with mm diameter were imbedded vertically on the curved surface. To prevent the pressure taps from interfering with one another, they were circumferentially positioned at 5–10 mm separation distances. The average pressure in a 10 s period was measured using a digital micro-manometer (Furness FC012).

The measurement technique in this study, described by Lee et al. [10, 11], provides a method for determining the surface isotherms using liquid crystals. By electrically heating a very thin gold coating on the Intrex, an essentially uniform wall heat flux condition is established. The heat flux can be adjusted by changing the current through the Intrex, which changes the surface temperature. Under the constant heat flux condition, an isotherm on the Intrex surface corresponds to a contour of a constant heat transfer coefficient. The local heat transfer coefficient at the position of the particular color being observed is calculated from

$$h = q_v / (T_w - T_j) \quad (1)$$

where, the net heat flux q_v is obtained by subtracting the heat losses from the total heat flux through the Intrex; i.e.

$$q_v = IV/A - \varepsilon\sigma(T_w^4 - T_a^4) - q_c \quad (2)$$

The variables $I, V, A, \varepsilon, \sigma, T_w, T_j, T_a$ and q_c are the current across the Intrex, voltage across the Intrex, surface area of the Intrex, emissivity of the liquid crystal and black paint coated surface (measured by infrared radiation thermometer: Minolta/505S), Stefan-Boltzmann constant, concave surface temperature measured by liquid crystal, jet temperature, ambient temperature and conduction loss through the back of the plate, respectively.

The Nusselt number uncertainty analysis on the basis of 20:1 odds (i.e. 95% confidence level of errors) has been carried out using the method by Kline and McClinton [12]. And the maximum uncertainty in the Nusselt number is estimated to be 4.5%.

3. Discussion of results

Figure 2 shows the profiles of the wall pressure coefficient C_p along the concave surface for $Re = 23\,000$. It should be noted that the wall pressure profiles for $Re = 11\,000$ and $50\,000$ are not shown here due to a similarity to those for $Re = 23\,000$ as well as a space limitation. In general, C_p monotonically decreases from

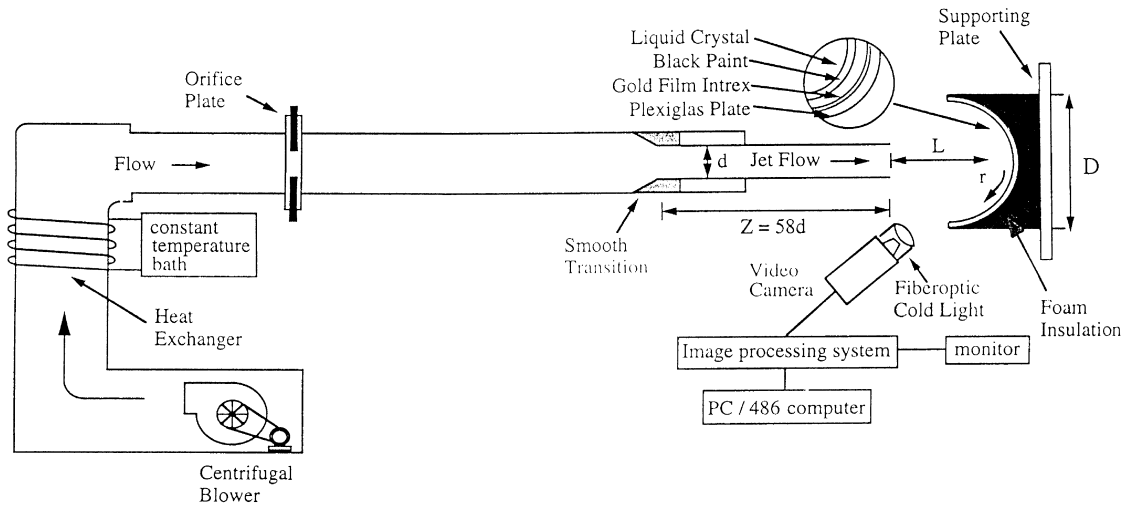


Fig. 1. Schematic diagram of the test apparatus for the jet impingement on the concave surface.

its maximum value at the stagnation point to zero C_p at $r/d \cong 3.8$. A value of C_p at the stagnation point for $L/d = 4$ is as high as 97% of that for $L/d = 2$, since the impinging surface is within the potential core length. For $L/d \geq 6$, C_p decreases significantly with L/d as the jet centerline velocity decays rapidly. It is also worthy to note that the profiles of C_p intersect at $r/d \cong 0.8$ for all Reynolds numbers tested. Beyond that point, the wall pressure appears to be unstable in the entire concave surface. A similar behavior reported by Thomann [5] that a boundary layer on a concave surface produces an unstable moment-of-momentum distribution because a particle displaced in the normal to the surface will not return to its original streamline.

The stagnation point Nusselt number (Nu_{st}) on the concave surface vs the dimensionless nozzle-to-surface distance (L/d) is plotted in Fig. 3 for different surface curvatures (d/D) and Reynolds numbers. It is observed that Nu_{st} increases with increasing surface curvature. The same heat transfer behavior for the wall jet region can also be deduced from the streamwise Nusselt number distributions (Figs 4–6). This behavior may be attributed to a thinning of the boundary layer caused by the surface curvature and a generation of Taylor–Görtler vortices. According to Thomann [5] and Schlichting [13], a centrifugal force created due to the curvature effect can destabilize the entire flow over the concave surface and produces series of large scale vortices with axes in the flow direction (called Taylor–Görtler vortices), which in turn increase the intensity of the turbulent mixing and enhance the heat transfer rate. Viskanta [3] has also suggested the initiation of Taylor–Görtler vortices along the concave surface and the heat transfer rate increases with increasing surface curvature.

Figure 3 also shows that Nu_{st} gradually increases with

increasing L/d and reaches a maximum at $L/d = 6$ for $Re = 11\,000$ and $23\,000$, and at $L/d = 8$ for $Re = 50\,000$ except for $d/D = 0.089$. It can be inferred that the location of the maximum Nu_{st} depends on both Reynolds number and the surface curvature (i.e. the lower Re and the larger surface curvature, the shorter potential core length). According to the flow data obtained by Lee et al. [9], the physical mechanism for the maximum Nu_{st} to occur at $L/d = 6–8$ is that not only the jet centerline velocity has not changed much from the initial centerline velocity, but the turbulence intensity reaches roughly a maximum value in that region.

Correlations of Nu_{st} in terms of Re , L/d and d/D are obtained as follows: $Nu_{st} = 1.7 (Re)^{0.47} (L/d)^{0.11} (d/D)^{0.2}$ for $2 \leq L/d < 6$, and $Nu_{st} = 1.74 (Re)^{0.56} (L/d)^{-0.37} (d/D)^{0.2}$ for $6 \leq L/d \leq 10$.

The above correlations are valid for $11\,000 \leq Re \leq 50\,000$ and $0.034 \leq d/D \leq 0.089$. It should be noted that for $2 \leq L/d < 6$, Nu_{st} varies according to $Nu_{st} \propto Re^{0.47}$, which approximately agrees with the $Re^{0.5}$ laminar boundary layer flow result and also agrees with the experimental results of Hoogendoorn [14] for the flat plate case. For the longer distances, the Reynolds number dependence is stronger ($Nu_{st} \propto Re^{0.56}$ for $6 \leq L/d \leq 10$). This is due to the fact that for $6 \leq L/d \leq 10$, the impinging surface is positioned outside of the potential core of the jet and a subsequent increase of the entrainment of the surrounding air to the jet flow has affected the heat transfer rate at the stagnation point region.

The local Nusselt number distributions along the concave surface are presented in Figs 4–6 for four nozzle-to-surface distances of $L/d = 2, 4, 6$ and 10 , three Reynolds numbers of $Re = 11\,000, 23\,000$ and $50\,000$, and three surface curvatures of $d/D = 0.034, 0.056$ and 0.089 . In general, the Nusselt number increases with increasing

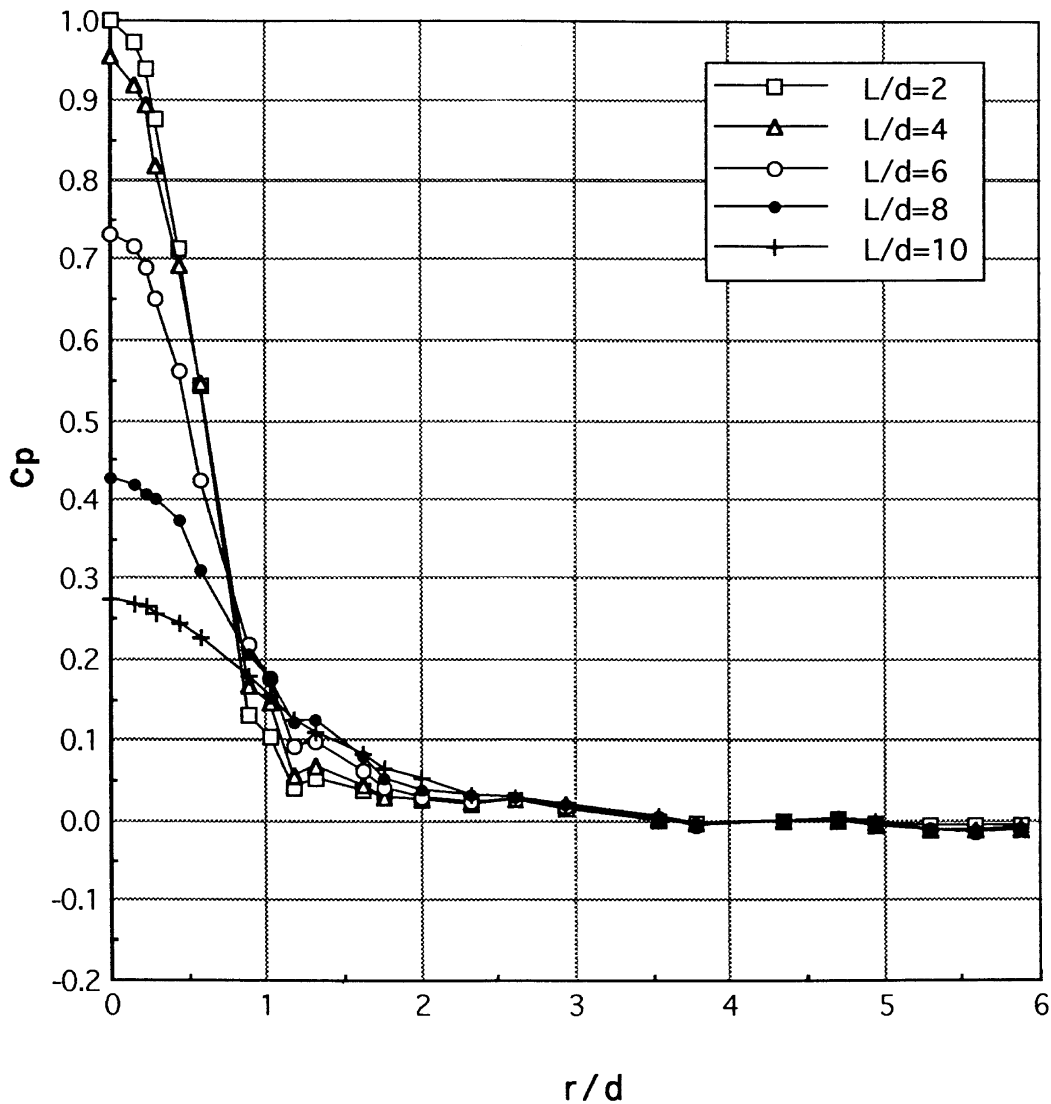


Fig. 2. Profiles of the wall pressure coefficient along the concave surface for $Re = 23\,000$ and $d/D = 0.089$.

Reynolds number and surface curvature. The Nusselt number monotonically decreases from its maximum value at the stagnation point up to $r/d \approx 1.0 \sim 1.5$.

For $Re = 11\,000$, a gradual reduction in the Nusselt number continues (beyond $r/d \approx 1.5$) as the thermal boundary layer thickness grows with r/d . However, Figs 4 and 5 show that for $L/d = 2$ and $Re = 23\,000$, and for $L/d \leq 4$ and $Re = 50\,000$, the local Nusselt number distributions exhibit increasing values in the region corresponding to $1.0 \leq r/d \leq 1.5$ and attain secondary maxima at $r/d \approx 2.0\text{--}2.2$. An occurrence of the secondary maxima in the Nusselt number is attributed to the fact that because the impinging surface is within the potential core region, the potential core of the jet flow impinges

upon the surface so that initially the laminar boundary layer develops from the stagnation point and a transition process takes place until the flow becomes turbulent at $r/d \approx 2.0\text{--}2.2$, resulting in a sudden increase in the heat transfer rate. Figures 4 and 5 show that the location of the secondary maxima looks independent of Reynolds number, the surface curvature, and the nozzle-to-surface distance. The same behavior has been observed in the impinging jet heat transfer study on the convex surface [9].

Secondary maxima have also been reported in the flat surface study by Yan [15] and in the concave surface study by Gau and Chung [7] at $r/d \approx 2$ for $L/d = 2$ and $23\,000 \leq Re \leq 70\,000$, and $r/b \approx 7$ for $Re = 11\,000$ and

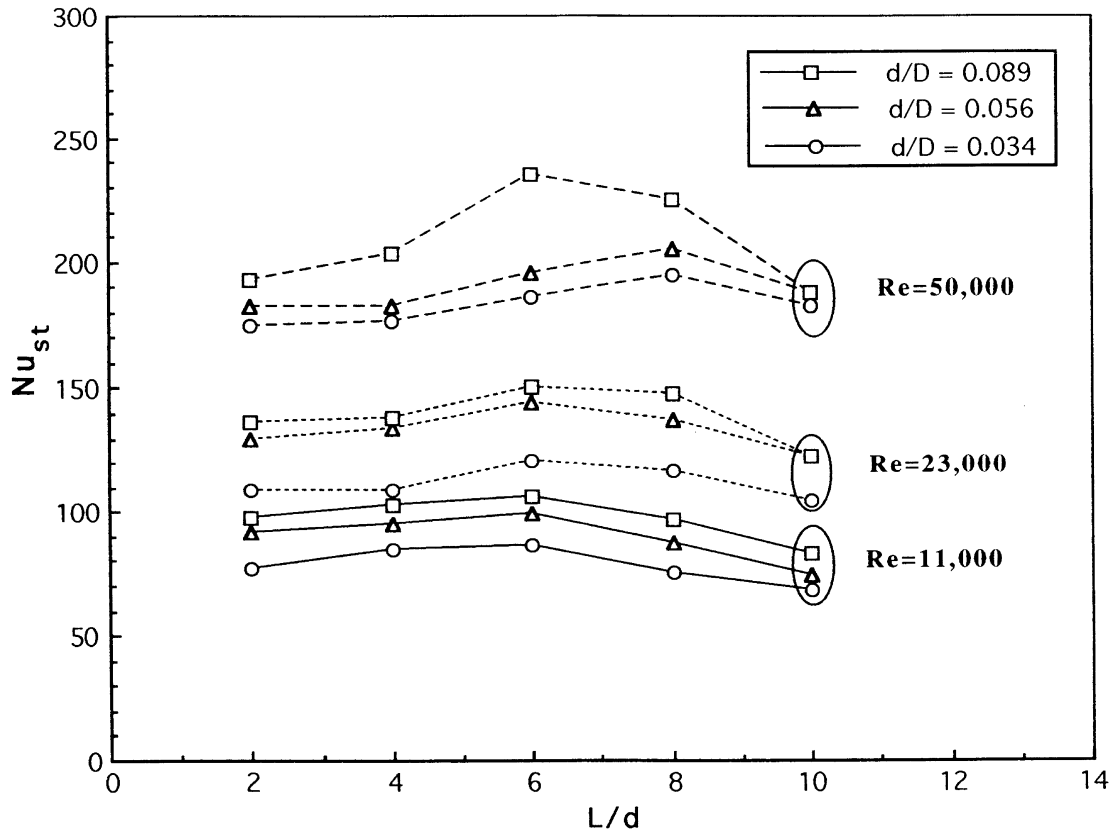


Fig. 3. Effect of Reynolds number and concave surface curvature on the stagnation point Nusselt number.

$Z/b = 4$ (where, Z/b is the dimensionless nozzle-to-surface distance for the two-dimensional slot jet), respectively. Yan [15] reported that as the Reynolds number increases from 23 000 to 70 000 the secondary maximum Nusselt number approaches the value at the stagnation point. In fact, our results in Fig. 4 show that for $Re = 50\,000$ and $d/D = 0.034$, the secondary maximum Nusselt number becomes greater than the stagnation point Nusselt number.

When the impinging surface is positioned outside of the potential core length (i.e. $L/d > 4$), a turbulence level in the jet flow approaching the surface is becoming high due to an increased entrainment of surrounding air to the jet flow. Therefore, a resulting higher Nusselt number at the stagnation point and a monotonic decrease of the local Nusselt number in the downstream region can be expected as shown in Fig. 6.

4. Conclusions

The experimental study has been carried out to investigate the effect of the hemispherically concave surface

curvature on the local heat transfer of a round impinging jet issuing from a long straight pipe nozzle. It was found that the Nusselt numbers for both stagnation point region and wall jet region increase with increasing surface curvature. This may be attributed to a thinning of the boundary layer caused by the surface curvature and a generation of Taylor-Görtler vortices, which in turn enhance the heat transfer rate.

For all values of Re and d/D tested, the maximum Nu_{st} occurs at $L/d \cong 6-8$ where not only a change in the jet centerline velocity from the initial velocity is small, but the turbulent intensity reaches roughly a maximum value in that region. The stagnation point Nusselt numbers are well correlated with Re , L/d and d/D . For $2 \leq L/d < 6$, the correlation agrees roughly with the $Re^{0.5}$ laminar boundary layer flow result. For the larger distances ($L/d \geq 6$), the Reynolds number dependence is stronger ($Nu_{st} \propto Re^{0.56}$). This may be due to an increase of turbulence levels in the approaching jet as a result of the stronger exchange of momentum with the surrounding air since the impinging surface is positioned outside of the potential core of the jet.

The local Nusselt number decreases monotonically

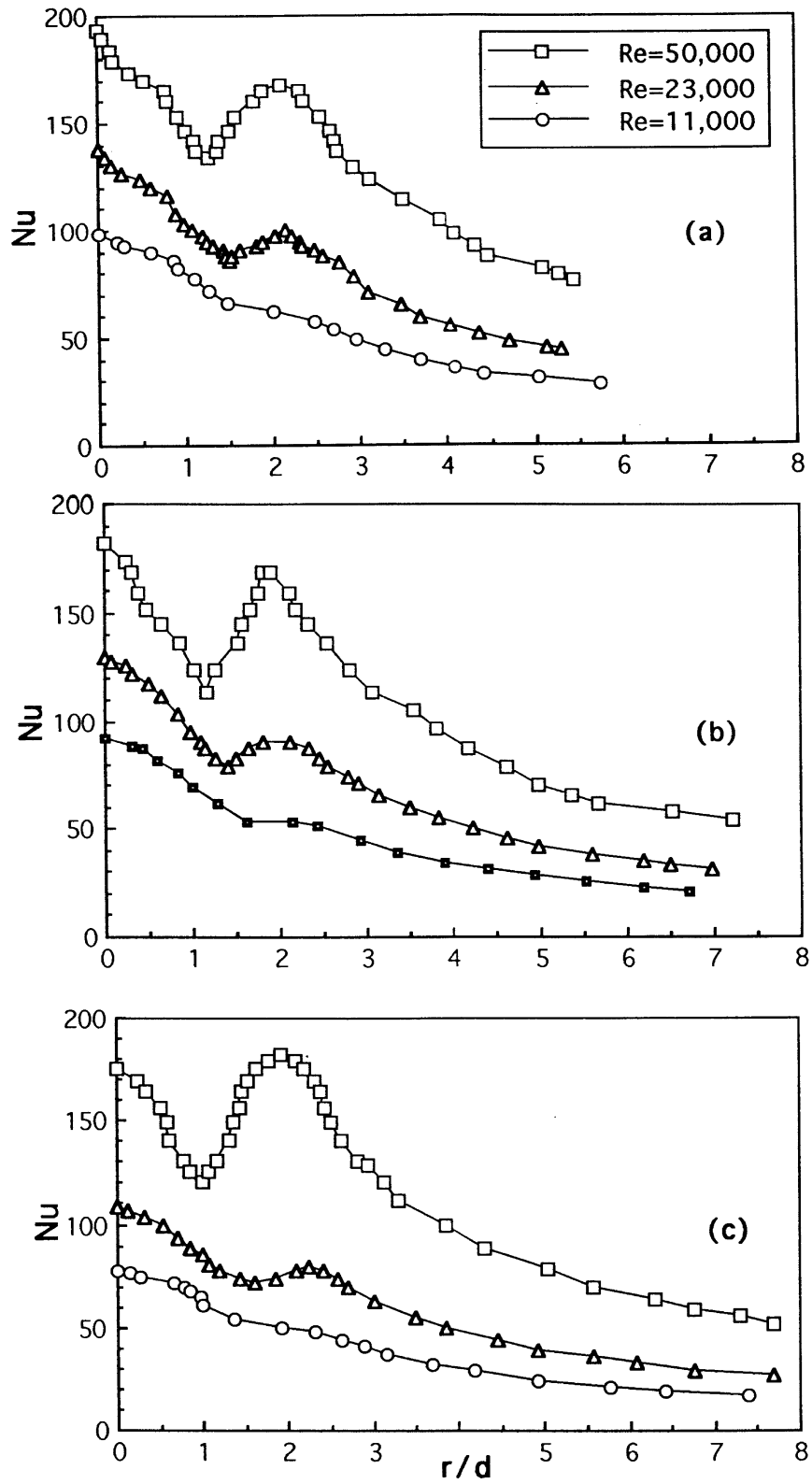


Fig. 4. Streamwise distributions of the local Nusselt number along the concave surface for $L/d = 2$: (a) $d/D = 0.089$; (b) $d/D = 0.056$; (c) $d/D = 0.034$.

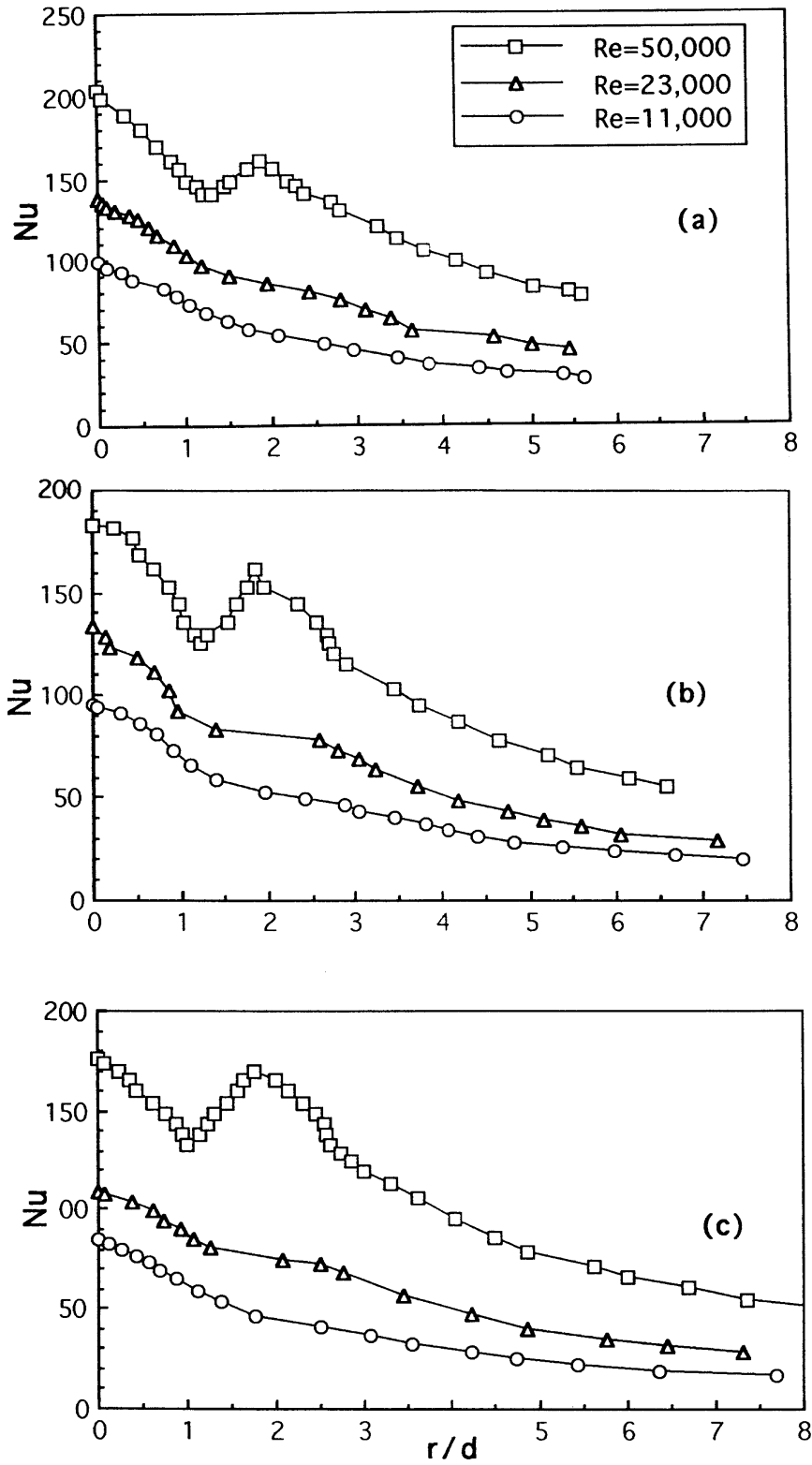


Fig. 5. Streamwise distributions of the local Nusselt number along the concave surface for $L/d = 4$: (a) $d/D = 0.089$; (b) $d/D = 0.056$; (c) $d/D = 0.034$.

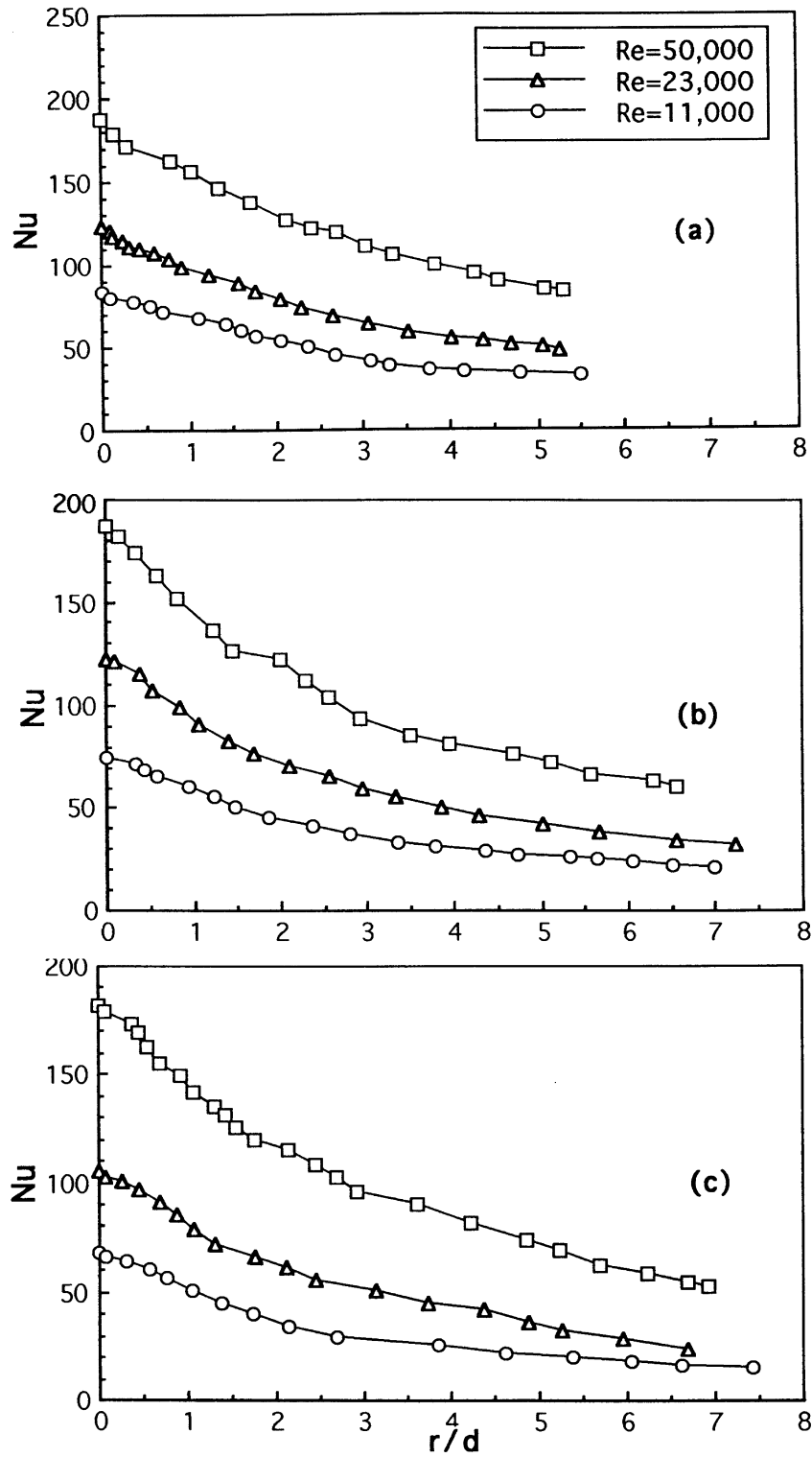


Fig. 6. Streamwise distributions of the local Nusselt number along the concave surface for $L/d = 10$: (a) $d/D = 0.089$; (b) $d/D = 0.056$; (c) $d/D = 0.034$.

from its maximum value at the stagnation point. However, for $L/d = 2$ and $Re = 23\,000$, and for $L/d \leq 4$ and $Re = 50\,000$, the local Nusselt number distributions exhibit increasing values in the region $1.0 \leq r/d \leq 1.5$ and attain secondary maxima at $r/d \cong 2.0$ – 2.2 . The formation of the secondary maxima is attributed to an increase in the turbulence level resulting from the transition from a laminar to a turbulent boundary layer.

References

- [1] H. Martin, Heat and mass transfer between impinging gas jets and solid surfaces, *Adv. Heat Transfer* 13 (1977) 1–60.
- [2] K. Jambunathan, E. Lai, M.A. Moss, B.L. Button, A review of heat transfer data for single circular jet impingement, *Int. J. Heat Fluid Flow* 13 (2) (1992) 106–115.
- [3] R. Viskanta, Heat transfer to impinging isothermal gas and flame jets, *Exp. Therm. Fluid Sci.* 6 (1993) 111–134.
- [4] R.E. Chupp, H.E. Helms, P.W. McFadden, T.R. Brown, Evaluation of internal heat transfer coefficients for impingement cooled turbine airfoils, *J. Aircraft* 6 (1969) 203–208.
- [5] H. Thomann, Effect of streamwise wall curvature on heat transfer in a turbulent boundary layer, *J. Fluid Mech.* 33 (1968) 283–292.
- [6] P. Hrycak, Heat transfer and flow characteristics of jets impinging on a concave hemispherical plate, *Proc. Int. Heat Transfer Conf.* 3 (1982) 357–362.
- [7] C. Gau, C.M. Chung, Surface curvature effect on slot-air jet impingement cooling flow and heat transfer process, *ASME J. Heat Transfer* 113 (1991) 858–864.
- [8] G.Y. Yang, M.S. Choi, J.S. Lee, An experimental study of jet impinging cooling on the semi-circular concave surface, *Trans. KSME J.* 19 (1995) 1083–1094.
- [9] D.H. Lee, Y.S. Chung, D.S. Kim, Turbulent flow and heat transfer measurements on a curved surface with a fully developed round impinging jet, *Int. J. Heat Fluid Flow* 18 (1997) 160–169.
- [10] D.H. Lee, R. Greif, S.J. Lee, J.H. Lee, Heat transfer from a flat plate to a fully developed axisymmetric impinging jet, *ASME J. Heat Transfer* 117 (1995) 772–776.
- [11] S.J. Lee, H. Lee, D.H. Lee, Heat transfer measurements using liquid crystal with an elliptic jet impinging upon the flat surface, *Int. J. Heat Mass Transfer* 37 (1994) 967–976.
- [12] S.J. Kline, F.A. McKlintock, Describing uncertainties in single sample experiments, *Mech. Engng.* 75 (1953) 3–8.
- [13] H. Schlichting, *Boundary Layer Theory*, 7th ed., McGraw-Hill, New York, 1979.
- [14] C.J. Hoogendoorn, The effect of turbulence on heat transfer at stagnation point, *Int. J. Heat Mass Transfer* 20 (1977) 1333–1338.
- [15] X. Yan, A preheated-wall transient method using liquid crystals for the measurement of heat transfer on external surfaces and in ducts, Ph.D. dissertation, University of California, Davis, 1993.